Divalent Cation Activation and Inhibition of Single Calcium Release Channels from Sheep Cardiac Sarcoplasmic Reticulum

R. H. ASHLEY and A. J. WILLIAMS

From the Department of Cardiac Medicine, National Heart and Lung Institute, University of London, London SW3 6LY, United Kingdom

ABSTRACT Single Ca^{2+} release channels from vesicles of sheep cardiac junctional sarcoplasmic reticulum have been incorporated into uncharged planar lipid bilayers. Single-channel currents were recorded from Ca^{2+}-activated channels that had a Ca^{2+} conductance of ~90 pS. Channel open probability increased sublinearly as the concentration of free Ca^{2+} was raised at the myoplasmic face, and without additional agonists the channels could not be fully activated even by 100 μM free Ca^{2+}. Lifetime analysis revealed a minimum of two open and three closed states, and indicates that Ca^{2+} activated the channels by interacting with at least one of the closed states to increase the rate of channel opening. Correlations between adjacent lifetimes suggested there were at least two pathways between the open- and closed-state aggregates. An analysis of bursting behavior also revealed correlations between successive burst lengths and the number of openings per burst. The latter had two geometric components, providing additional evidence for at least two open states. One component appeared to comprise unit bursts, and the lifetime of most of these fell within the dominant shorter open-time distribution associated with over 90% of all openings. A cyclic gating scheme is proposed, with channel activation regulated by the binding of Ca^{2+} to a closed conformation of the channel protein. Mg^{2+} may inhibit activation by competing for this binding site, but lifetime and fluctuation analysis suggested that once activated the channels continue to gate normally.

INTRODUCTION

The intracellular switch controlling the release of Ca^{2+} from the sarcoplasmic reticulum (SR), and triggering skeletal and cardiac muscle contraction, could involve intermembranous charge transfer (Schneider and Chandler, 1973), Ca^{2+}-induced Ca^{2+}release (Endo, 1981), or a chemical link such as inositol trisphosphate (Volpe et al., 1985). As a final common pathway only gated membrane channels could release

Address reprint requests to Dr. Richard Ashley, Department of Biochemistry, University of Edinburgh Medical School, Hugh Robson Building, George Square, Edinburgh, Scotland EH8 9XD, United Kingdom.

J. GEN. PHYSIOL. © The Rockefeller University Press · 0022-1295/95/05/0981/25 $2.00
Volume 95 May 1990 981–1005

Ca^{2+} sufficiently quickly, and the search for channels in SR membranes prompted some pioneering reconstitution experiments (Miller and Racker, 1976) leading, several channels later, to Smith et al. (1985) making the first convincing recordings of a "Ca^{2+} release" channel. Interestingly, myoplasm Ca^{2+} and Mg^{2+} are important physiological modulators of this channel in both skeletal (Meissner, 1984; Smith et al., 1986) and cardiac muscle (Meissner and Henderson, 1987; Rousseau et al., 1986).

The apparent delay in demonstrating the channel was partly due to its rather specific location in relatively minor membrane fractions: skeletal terminal cisternal (and equivalent cardiac junctional) membranes (Imagawa et al., 1987). These also contain large numbers of Cl^--selective channels, and the creation of a Cl^- gradient across the vesicularized membrane, with subsequent entry of Cl^- and water, may be crucial for vesicle swelling and fusion (Finkelstein et al., 1986; Woodbury and Hall, 1988) with a preformed bilayer (Smith et al., 1985). The Ca^{2+} release channel can then be observed by changing the solutions bathing the membrane, but again there is evidence that too much Ca^{2+} can inactivate the channel in some circumstances (Smith et al., 1986). The experiments reported here were performed under conditions very similar to those described by Meissner and his colleagues (Rousseau et al., 1986; Smith et al., 1985, 1986), the main differences lying in the choice here of a neutral bilayer, the avoidance of agonists other than divalent cations, and a strict requirement for only single-channel incorporation.

The cardiac channel differs from the skeletal channel not only in having a lower conductance of Ca^{2+} but also in being more dependent on calcium, rather than adenine nucleotides, for activation (Rousseau et al., 1986). Modelling the functional interactions of Ca^{2+} (and Mg^{2+}) with the myoplasmic face of the cardiac channel may suggest ways in which the cations could interact with the purified channel protein (Imagawa et al., 1987; Lai et al., 1988 *a*, *b*). A standard Markov scheme, involving a limited number of discrete states, is postulated. A fractal analysis (Liebovitch et al., 1987) was not pursued because limited time resolution precluded a valid statistical comparison between Markov and fractal schemes. It was impossible to activate the channel fully with Ca^{2+} alone, although kinetic analysis suggested that Ca^{2+} could bind to a single nonconducting conformation of the channel protein to initiate a cyclic or branched gating scheme which included at least two open and another two closed states. Mg^{2+} may inactivate the channel simply by competing with Ca^{2+} for this binding site.

METHODS

General Methods

SR vesicles were prepared from sheep ventricular muscle in the presence of 1 mM PMSF, using a subcellular fractionation procedure based on that described for canine cardiac muscle (Meissner and Henderson, 1987). Microsomal suspensions were centrifuged for 2 h at 150,000 g_{max} through discontinuous density gradients comprising 10, 20, 30, and 40% (wt/wt) sucrose and membrane vesicles were pelleted from a well-defined band which appeared at the 30–40% interface. These membranes, corresponding to Meissner's "heavy sarcoplasmic reticulum" vesicles (HSR), will be called "sheep heavy sarcoplasmic reticulum" vesicles (SHSR). Aliquots in 0.4 M sucrose were frozen in liquid N_2 and stored for up to 3 mo at −80°C at a protein concentration (Lowry et al., 1951) of 5 mg/ml.

Lipid bilayers were cast from phosphatidylethanolamine (PE; Avanti Polar Lipids, Birmingham, AL), dispersed in *n*-decane (30 mg/ml). The membranes were allowed to thin across a 300-μm hole in a polystyrene partition separating two solution-filled chambers and were voltage-clamped by using standard operational amplifier circuitry, with frequency compensation (Sigworth, 1983). Thinning was monitored by light reflectance and capacitance. Black, fully thinned membranes had capacitances of 250–300 pF (and resistances of 20–100 GΩ). The voltage drop across the feedback resistor (10 mV/pA of transmembrane current with a 10-GΩ high precision resistor from K & M Electronics, W. Springfield, MA) was digitized by a modified audio processor (16 bit, DC to 20 kHz), after subtracting the clamp voltage, and stored on videotape.

SHSR vesicles were fused with bilayers at room temperature under the conditions described by Smith et al. (1986). Briefly, up to 5 μl of thawed SHSR vesicles were stirred into one (500 μl) chamber, thus defining the *cis* side, while both *cis* and *trans* chambers contained 50 mM choline chloride, 2–5 mM calcium chloride, 100 μM diethylenetriaminepenta-acetic acid (DPA) and 10 mM Tris/HEPES (pH 7.4). The concentration of choline chloride in the *cis* chamber was then increased to at least 250 mM (by additions from a concentrated stock solution in the same buffer). If an osmotic gradient did not promote fusion within 20 min, with the appearance of Cl^--selective channels, the chambers were rinsed out and the whole process was repeated. Many (though not all) of the Cl^- channels were similar to those observed in skeletal muscle SR (Tanifuji et al., 1987).

After monitoring fusion events in this way the contents of both chambers were replaced by new solutions. The *cis* chamber was stirred and perfused with 10 vol of 125 mM Tris/250 mM HEPES (pH 7.4) containing 110 μM calcium chloride (or gluconate) and 10 μM DPA. The *trans* solution was displaced (Smith et al., 1986) by 3 vol of 250 mM HEPES containing calcium hydroxide, added to a pH of 7.4 (divalent cation concentration 54 mM). If the fused vesicles had also dumped Ca^{2+} release channels into the bilayer, currents of ~3 pA now flowed *trans-cis* while the bilayer was clamped at 0 mV.

The SR vesicles that fuse with bilayers are almost always right-side-out (Miller and Rosenberg, 1979). Therefore, the myoplasmic side of incorporated channels faced the *cis* chamber and the SR lumenal side faced *trans*. The free Ca^{2+} concentration on the *cis*, cytoplasmic, side was reduced by extensive perfusion of the *cis* chamber with fresh solutions containing 1 mM EGTA. Calcium chloride or gluconate were included in the perfusate, or occasionally added to the *cis* solution, and free Ca^{2+} concentrations were calculated from the appropriate absolute, and mixed proton association constants for all the relevant species (Blinks et al., 1982), using an iterative computer program.

Experiments were only carried out on channels that were sensitive to the concentration of calcium in the *cis* chamber. The Ca^{2+}-insensitive channels which were occasionally seen were regarded as a distinct channel type or modification. Only channels with a (slope) conductance of ~90 pS for Ca^{2+} were investigated. Other unit conductances or substates were seen infrequently. 90-pS channels with prominent substates (which were often Ca^{2+} insensitive) were also rejected. More of these were seen after leaving vesicles on ice for longer than ~8 h. Unless noted otherwise, all recordings were made at a holding potential (*cis-trans*) of 0 mV.

Analysis

Recordings were replayed in analogue format and low-pass filtered using a Krohn-Hite 3200R 4-pole filter (Avon, MA) in "RC"-mode at a front-panel setting of 0.4 kHz. Data for fluctuation analysis were filtered with a Butterworth-type response (−3 dB at half the sampling frequency). The filtered recordings were redigitized at 20 kHz for analysis using an Indec/LSI-11/73 laboratory computer (Indec, Sunnyvale, CA) or an Intracel/AT system (Intracel, Cambridge, UK).

Channel open probability (P_o) was measured by integrating steady-state amplitude histograms from contiguous 3-min recordings. These current records were also observed on an oscilloscope and a single active channel was considered to be present if, at some stage in the experiment, only one open level was seen over a period of at least 20 s during which P_o approached 1 (favored by 100 μM *cis* Ca^{2+}, especially with 1 mM ATP or adenosine 5′-(β, γ-methylene) triphosphate, and a holding potential of +30 mV, cf. Smith et al., 1986). Some of these single-channel records were subjected to lifetime and burst analysis.

For standard lifetime analysis the cut-off frequency (f_c) of the RC-mode filter was chosen as follows. Initially, channel sizes (estimated from the means of amplitude histograms after filtering the data at 0.2–0.4 kHz) allowed definition of a value midway between closed and open current levels for half-amplitude threshold analysis. Current records from the same bilayer, prefusion, were then analyzed for threshold crossings. f_c = 0.4 kHz was (just) sufficient to prevent bilayer noise from being falsely recognized as channel openings (or closures) in the noisiest records examined, and was not increased for quieter recordings (so the records remained comparable). During lifetime analysis the entire record (normally at least 3 min) was inspected in detail, and in all the records examined, <2% of openings were to subconductance levels (too few to affect the results).

Channel lifetimes measured by half-amplitude threshold analysis were stored in sequential files and grouped into (noncumulative) histograms for display on linear scales. Individual times (t) were fitted to a probability density function (PDF) containing up to three exponential terms,

$$\text{PDF} = f(t) = \sum_{j=1}^{k} a_j/\tau_j \cdot \exp(-t/\tau_j) \tag{1}$$

numerically optimizing the values for areas a_j ($\Sigma a_j = 1$) and time constants τ_j which maximized the probability of obtaining the observed set of data (Colquhoun and Sigworth, 1983). In practice, the PDF was calculated as the sum of log (likelihoods). For f_c = 0.4 kHz, openings or closures lasting <1 ms failed to cross the 50% threshold for detection, and events lasting between 1 and 2 ms were attenuated. Therefore all lifetimes lasting <2 ms were excluded from the fitting procedure and the correction described by Colquhoun and Sigworth (1983) was applied, so that

$$f(t) = \frac{\sum_{j=1}^{k} a_j/\tau_j \cdot \exp(-t/\tau_j)}{\sum_{j=1}^{k} a_j[\exp(-t_{\min}/\tau_j) - \exp(-t_{\max}/\tau_j)]} \tag{2}$$

where the distribution in Eq. 1 is divided by the probability that an observation lies between $t_{\min}$ (the minimum resolvable lifetime, 2 ms) and $t_{\max}$ (the maximum period of observation). The true number of events (N) could be found by correcting the observed number, n, appropriately:

$$N = n/\sum_{j=1}^{k} a_j[\exp(-t_{\min}/\tau_j) - \exp(-t_{\max}/\tau_j)] \tag{3}$$

Although the closed-time distributions clearly included more than one exponential component (see Results), bursting behavior was rarely obvious because the closed-time constants were insufficiently well-separated. Bursts of openings were therefore defined by calculating a minimum interburst interval, T, such that:

$$a_s \cdot \exp(-T/\tau_s) = \sum_{l=1}^{k} a_l[1 - \exp(-T/\tau_l)] \tag{4}$$

τ_s and a_s, or τ_l and a_l, were the time constants and areas characterizing the very shortest and the (one or two) longer components, respectively. This procedure was similar to that of Magleby and Pallotta (1983) and resulted in the misclassification of equal numbers of short and long closures, to an extent discussed in due course.

Histograms of interburst intervals and burst durations were also fitted to one or two exponential terms. Multiexponential fits were very obvious, and in these cases fitting was more easily performed by eye as the absolute values of the τ and a parameters were not important. The numbers of openings per burst were fitted to geometric distributions:

$$P(r) = \sum_{j=1}^{k} a_j(1 - \rho_j)\rho_j^{r-1} \tag{5}$$

where $P(r)$ is the probability of obtaining r openings in a burst, a_j are the relative areas of the distribution ($\Sigma a_j = 1$), and the parameters ρ_j are each <1. For >1 component the maximum likelihood values for a_j and ρ_j were found by using a numerical procedure similar to that described for lifetime analysis. For the discrete distributions, the overall time resolution was effectively doubled since within a burst only threshold crossings, rather than fully resolved events, were important. Any closure long enough by definition to terminate a burst was always long enough to be fully resolved.

Autocorrelation analysis (Labarca et al., 1985) and the runs test (Colquhoun and Sakmann, 1985) were carried out on sequential lifetime and burst-length files, to investigate connectivity (Colquhoun and Ogden, 1986). The autocorrelation coefficient for the k'th opening (or closure, or burst length) along, r_k, was estimated from the original observations, $y_i (i = 1, 2, \ldots, N$, mean $\bar{y})$, as

$$r_k = \frac{\sum_{i=1}^{n-k} (y_i - \bar{y})(y_{i+k} - \bar{y})}{\sum_{i=1}^{n} (y_i - \bar{y})^2} \tag{6}$$

The 95% confidence limits for the absence of correlation were placed at $-N^{-1} \pm 2N^{-0.5}$ (Kerry et al., 1987). Autocorrelation function decay was analyzed as the sum of $N_p - 1$ geometrically decaying components, where N_p pathways link the open and closed states (Kerry et al., 1987).

Data were examined for runs by dividing a sequence of events into two categories around a chosen critical length. For example, with two categories 0 and 1, the sequence 0110001 contains four runs. After counting the number of runs (T) for the critical length l (l was systematically varied as described later) the test statistic $Z(l)$ was determined as

$$Z(l) = [T - E(T)]/[\text{var}(T)]^{0.5} \tag{7}$$

The mean and variance of T, $E(T)$, respectively, and var(T) being defined as

$$E(T) = \frac{2n_0n_1}{N} + 1 \tag{8}$$

$$\text{var}(T) = [2n_0n_1(2n_0n_1 - N)]/N^2(N - 1) \tag{9}$$

where N, n_0, and n_1 are the total number of events and the numbers in categories 0 and 1, respectively. $Z(l)$ is in effect a standardized random variable with a mean of 0 and a variance of 1.

For fluctuation analysis recordings from the same bilayers, before and after vesicle fusion, were filtered at 2 kHz (−3 dB cut-off, Butterworth-type response) and sampled every 250 μs to accumulate a total of 6,400–12,800 data points. Spectral densities were obtained by using a Fourier transform program.

RESULTS

General Characteristics of Reconstituted Channels

The reconstituted channels were similar to those described previously in canine cardiac SR membranes (Rousseau et al., 1986, 1987). Some comparable data are summarized in Fig. 1 *A*, which shows how 100 μM Ca^{2+} with 1 mM ATP caused near-maximal activation of one channel (traces on right) and also illustrates the "gear-shift" phenomenon which the Ca^{2+} channel shares with some Ca^{2+}-activated K^+

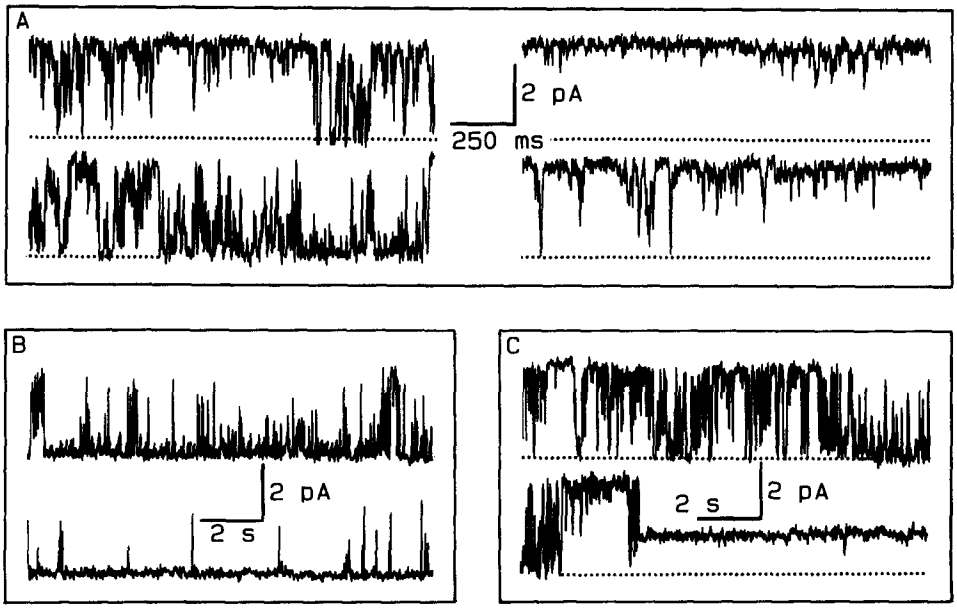

FIGURE 1. Single Ca^{2+} channel properites. Recordings were obrained under the conditions described in the text. All openings are upwards, and dotted lines mark the closed level where necessary. In *A* the left-hand pair traces represent a continuous 3.2-s segment of a recording from a channel activated by 100 μM Ca^{2+}. The right-hand pair of traces represent another continuous segment of data from the same channel after adding 1 mM ATP to the *cis* chamber. *B* shows another channel activated by 10 μM Ca^{2+} (*upper trace*). This was blocked immediately after adding 1 mM ruthenium red to the *cis* chamber (*lower trace*). In *C* a third single channel, activated by 100 μM Ca^{2+}, is shown "locked" into a subconductance state 3.2 min after adding 5 μM ryanodine to the *cis* chamber.

channels (Moczydlowski and Latorre, 1983; Moczydlowski, 1986). The channel in the control left-hand pair of traces switches from being mainly open, with occasional closures, to mainly closed, with occasional openings (the more common gating state).

Both ruthenium red and ryanodine had characteristic effects on the reconstituted channels. Fig. 1 *B* shows how 1 μM ruthenium red, added to the myoplasmic face of a channel activated by 10 μM Ca^{2+}, caused an apparent slow block with a dramatic decrease in channel opening. The alkaloid ryanodine (*C*) "locked" channels into a

mainly open subconductance state of ~40% of the main open level (Rousseau et al., 1987). Once modified, channels did not revert to their original behavior, even 60–90 min after reperfusion with ryanodine-free solutions.

Channel P_o

Measurements of single-channel P_o, made from records such as those in Fig. 2 *A*, provided the most fundamental assessment of Ca^{2+} activation. Any time-inhomogeneity caused by gearshifting appeared to be overcome by analyzing contiguous recordings lasting at least 3 min. Because <10% of all vesicle fusions led to the incorporation of a single Ca^{2+} release channel, and it was rarely possible to change *cis* (myoplasmic) free [Ca^{2+}] more than four or five times with each bilayer before breakage (giving a total recording time of up to ~20 min), the results from several

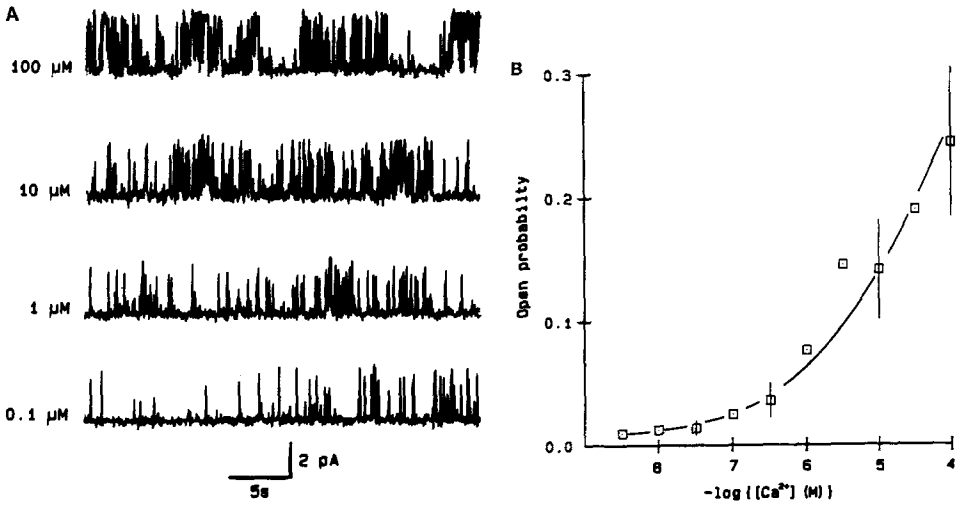

FIGURE 2. Open probability and activating free [Ca^{2+}]. (*A*) 32-s recordings from a single channel activated by 0.1–100 μM Ca^{2+} (opening upwards). (*B*) Mean data from several single-channel experiments showing ± SD only where at least six single-channel experiments were combined.

experiments were combined for Fig. 2 *B*. Open probabilities are summarized as [Ca^{2+}] is increased over more than 4 orders of magnitude, and clearly P_o increases sublinearly with agonist concentration (the curve obeying the approximate relationship $P_o \propto [Ca^{2+}]^{0.3}$). When it was possible to examine individual channels over a wide range of free [Ca^{2+}], commonly pCa 4–8, the same response was observed. Ba^{2+} at up to 1 mM failed to further activate channels exposed to 10 μM free [Ca^{2+}], suggesting a Ca^{2+}-specific effect. Inhibition by Mg^{2+}, which was accompanied by a marked reduction in P_o, is described in detail later.

In some experiments *cis* free [Ca^{2+}] was increased beyond 100 μM, but single-channel currents activated by 1–10 mM Ca^{2+} could only be satisfactorily resolved with much heavier filtering (front panel settings as low as 0.1 kHz). With 1 mM activating Ca^{2+} P_o was 0.18 ± 0.09 (mean ± SD, $n = 4$). Given the approximate rela-

tionship between P_o and free [Ca^{2+}] already noted, concentrations of 1–10 mM should have led to a P_o close to 1. In fact, for any given channel it appeared to be impossible to drive P_o to 1 at a holding potential of 0 mV using Ca^{2+} alone, and Smith et al. (1986) have reported that high concentrations of Ca^{2+} actually inactivated Ca^{2+} release channels from skeletal muscle. Because of the limitations imposed by filtering and the need for comparable channel analysis, this study could not be extended in detail beyond 100 μM activating Ca^{2+} (a level already well beyond the physiological range). It was however noted that channel amplitudes decreased significantly with 1–10 mM *cis* Ca^{2+}, and although this may have been a straightforward consequence of the reduced electrochemical gradient for Ca^{2+} (and there was a small shift in reversal potential) it is possible that high myoplasmic calcium concentrations did cause self-block.

Lifetime Distributions after Ca^{2+} Activation

Ca^{2+}-activated cardiac Ca^{2+} release channels always had at least three closed and two open states. Fig. 3 shows lifetime distributions and channel openings on a fast time scale from the same channel with both low (0.1 μM) and high (100 μM) activating Ca^{2+}. Fits to single, double, and triple exponentials (Eq. 2) were compared by using the likelihood ratio test (Horne and Lange, 1983; Blatz and Magleby, 1986*a*), calculating the χ^2 statistic as $2[\ln(Lx - \ln(Ly)]$, where Lx and Ly were the likelihoods of the two fits being compared. The number of degrees of freedom was equal to the difference in the number of independent parameters in the two distributions. Channel open times were always better fitted by two exponential components rather than one ($P < 0.05$), but the differences in χ^2 between two and three components were not statistically significant. However, additional open and closed states may have been overlooked either because their lifetimes overlapped or because they contributed too few events to be noticed. Finally, 15–20% of all openings and 10–15% of all closures were missed because of the limited time resolution (a dead time of 1 ms), and states with mean lifetimes of <2 ms may remain undetected.

Ca^{2+} activated the channels by interacting with one or more closed conformations of the channel protein (Figs. 3 and 4). This increased the opening rate and thence P_o. Open channels (and therefore closing rates) were unaffected. Fig. 4 summarizes typical mean closed times obtained from a single channel where [Ca^{2+}] was increased from 0.01 to 100 μm. All the mean closed times were reduced by Ca^{2+}, but approached limiting values (of ~3, 10, and 30 ms in the example shown) above

FIGURE 3. (*opposite*) Single-channel lifetimes with low (*left-hand column*) and high (*right-hand column*) activating free Ca^{2+}. (*A*) examples of single-channel currents showing closed (lower) and open (upper) cursor levels. Events must last at least 2 ms to be fully resolved. (*B*) open and (*C*) closed lifetime histograms are combined with PDFs fitted by maximum likelihood (with missed events correction) to the individual lifetimes. The open time PDFs for this channel are $f(t) = 0.95/2.7 \cdot \exp(-t/2.7) + 0.05/15 \cdot \exp(-t/15)$ with 0.1 μM Ca^{2+} and $f(t) = 0.90/2.7 \cdot \exp(-t/2.7) + 0.10/13 \cdot \exp(-t/13)$ with 100 μM Ca^{2+}. The corresponding closed time PDFs are $f(t) = 0.33/11 \cdot \exp(-t/11) + 0.43/46 \cdot \exp(-t/46) + 0.24/137 \cdot \exp(-t/137)$ and $f(t) = 0.48/5.4 \cdot \exp(-t/5.4) + 0.40/13 \cdot \exp(-t/13) + 0.12/44 \cdot \exp(-t/44)$, respectively (all time constants are in milliseconds).

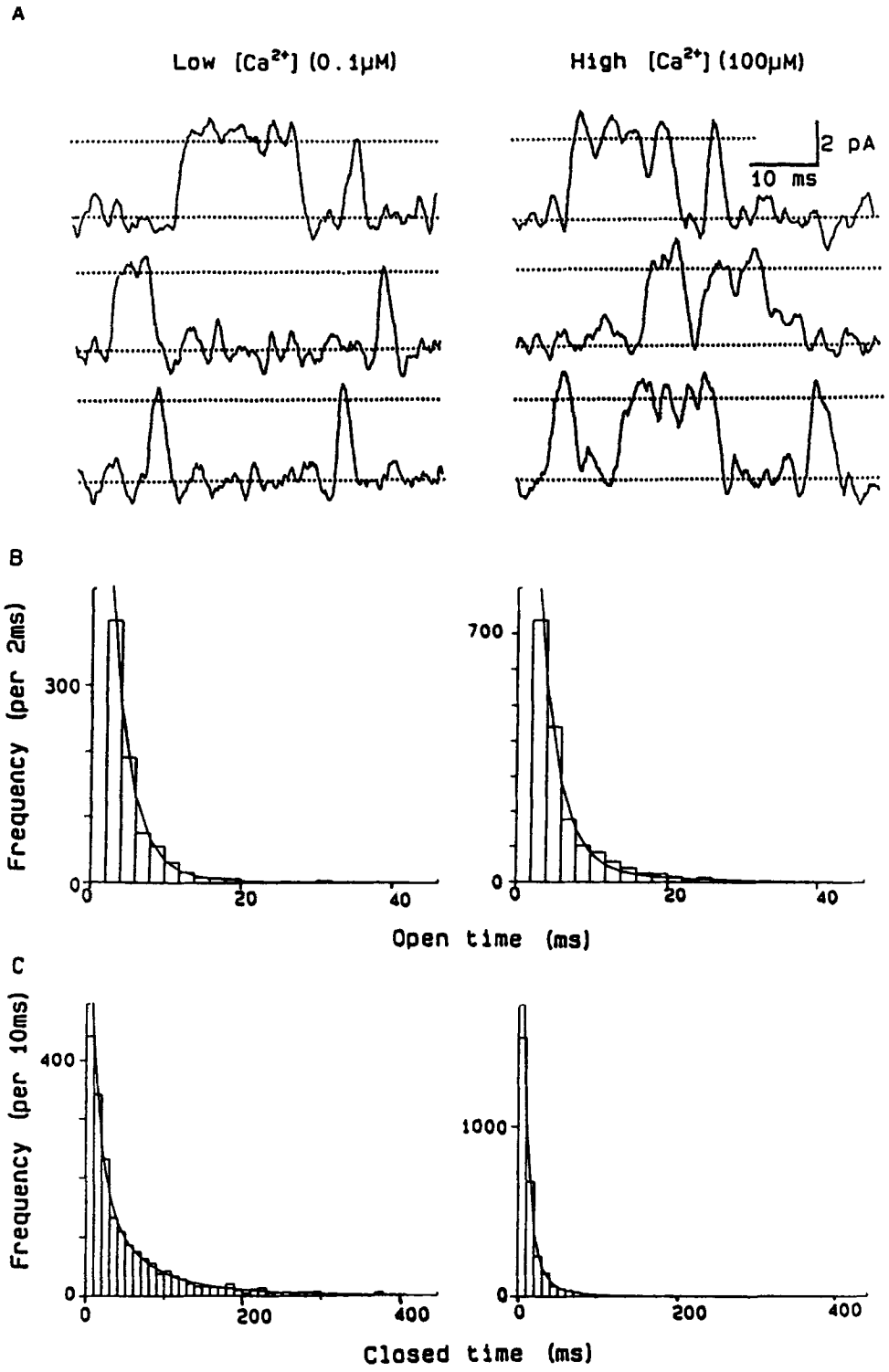
A
Low [Ca2+] (0.1μM)
High [Ca2+] (100μM)
2 pA
10 ms
B
Frequency (per 2ms)
300
0
0
20
40
700
0
0
20
40
Open time (ms)
C
Frequency (per 10ms)
400
0
0
200
400
1000
0
0
200
400
Closed time (ms)

FIGURE 3.

100 μM. Lifetime parameters for several channels are combined in Table I. Open lifetimes remained the same despite the marked variation in free [Ca^{2+}], the shorter mean lifetime lying close to 2–3 ms and the longer having a mean of 23 ± 7 ms (+SD of all 22 measurements). Over 90% of all openings were to the short lifetime distribution, whatever the value of free [Ca^{2+}]. The same table shows how the closures remained approximately equally divided between those to the very shortest-lived distribution and those to the two longer-lived distributions. The longest-lasting

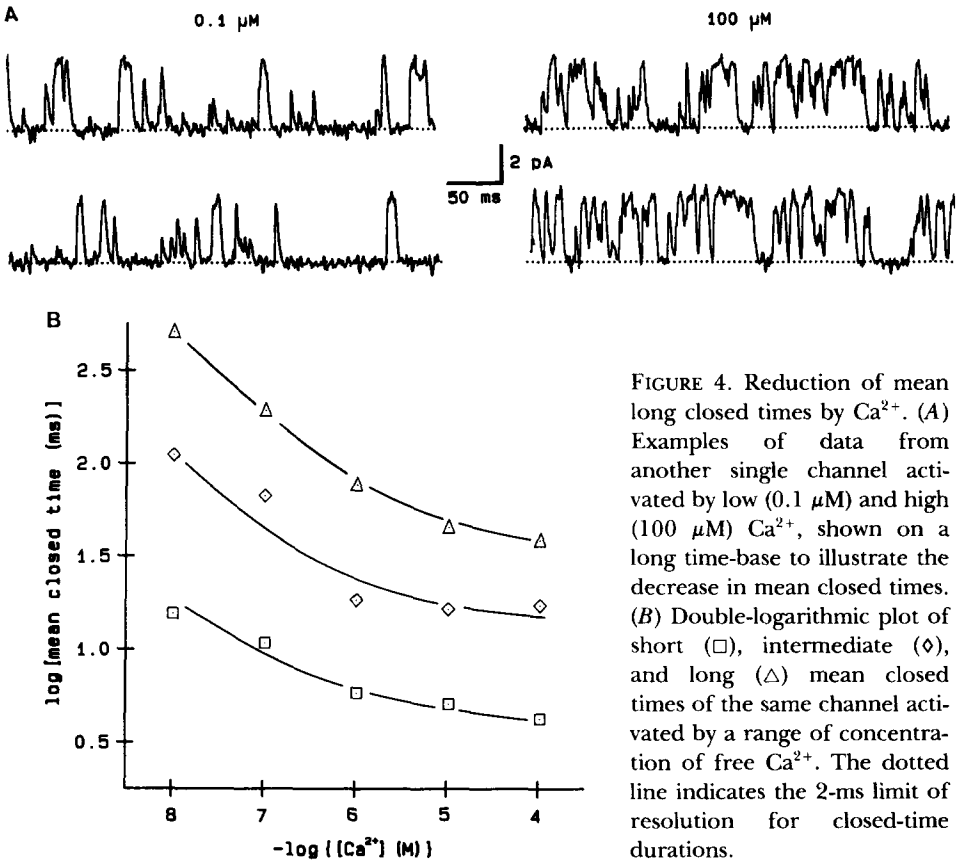

FIGURE 4. Reduction of mean long closed times by Ca^{2+}. (*A*) Examples of data from another single channel activated by low (0.1 μM) and high (100 μM) Ca^{2+}, shown on a long time-base to illustrate the decrease in mean closed times. (*B*) Double-logarithmic plot of short (□), intermediate (◇), and long (△) mean closed times of the same channel activated by a range of concentration of free Ca^{2+}. The dotted line indicates the 2-ms limit of resolution for closed-time durations.

closures always comprised a relatively small (though significant) proportion of events.

Average Properties of Bursts of Openings

The existence of multiple closed states necessarily gave rise to bursting behavior, where resistance of the channels in longer-lasting closed states (interburst intervals) interrupted sequences of shorter-lived closures (gap within bursts). Some preliminary information was obtained about Ca^{2+} and the average properties of bursts by equating the area under the shortest-lived component of the closed-time distribu-

tion to gaps within bursts, and the area under longer components to interburst intervals (Colquhoun and Sigworth, 1983).

The mean number of gaps per burst was calculated from the data for individual channels as the relative number of gaps within bursts divided by the relative number of interburst intervals i.e., $a_s/\Sigma a_l$. The value did not change systematically with $[Ca^{2+}]$, and from the experiments summarized in Table I the overall mean was 135 ± 82 gaps per 100 bursts (±SD, $n = 22$). Similarly, the mean burst length was found by dividing the total open time (mean open time × number of openings) by the number of bursts (Σa_l × number of closures), i.e., mean open time/Σa_l. It was previously noted that open lifetimes and the areas of closed-time distributions were

TABLE I

Channel Lifetime Parameters

$[Ca^{2+}]$	Open lifetime distribution		Closed lifetime distribution	
	Time constant	Area	Time constant	Area
μM	*ms*	%	*ms*	%
0.01 (n = 3)	3.0 (1.2)	88 (6)	16 (5.8)	45 (7)
	21 (2.2)	12 (6)	151 (60)	41 (9)
			473 (42)	14 (9)
0.10 (n = 5)	2.5 (0.4)	94 (3)	8.4 (2.7)	38 (16)
	24 (9.9)	6 (3)	53 (9.2)	39 (15)
			224 (58)	23 (15)
1.00 (n = 4)	3.3 (0.8)	94 (2)	5.2 (0.8)	50 (10)
	22 (9.3)	6 (2)	21 (1.8)	42 (11)
			96 (12)	8 (3)
10.0 (n = 5)	3.8 (1.3)	91 (8)	4.8 (0.8)	61 (7)
	27 (3.0)	9 (8)	17 (3.6)	32 (6)
			51 (7.1)	7 (3)
100 (n = 5)	3.2 (0.9)	90 (5)	4.4 (0.9)	65 (11)
	20 (4.3)	10 (5)	18 (1.9)	29 (8)
			49 (7.3)	6 (3)

Mean values (each from n = 3–5 channels, ±SD in parentheses) are maximum likelihood fits to single-channel data.

little affected by Ca^{2+}, and as expected the mean burst length did not appear to vary either (9.3 ± 3.8 ms, ± SD, $n = 22$).

Burst Distributions

The actual distributions of burst lengths and the numbers of openings per burst were likely to be much more informative. However, the means (and therefore SDs) of all three closed-time distributions lay very close together for these channels, making bursts difficult to separate. A minimum interburst interval was therefore chosen by using the criterion outlined in the Methods section, so that incorrectly assigned closed intervals were drawn in equal numbers from "true" interburst intervals and "true" gaps within bursts. The fact that closed lifetime analysis had shown for individual channels a fairly constant and often broadly equal division of closed times

between the shortest and two longer distributions helped to justify this approach in that on the whole the same proportions as well as the same numbers of closed times were misclassified. Overall the mean number of openings per burst (which changed hardly at all, as described earlier) should have remained relatively undistorted by this procedure. Another approach is given by Colquhoun and Sakmann (1985).

Fig. 5 illustrates typical cumulative histograms of interburst intervals and burst durations obtained by analyzing a single channel activated by 100 μM free Ca^{2+}. The (maximum likelihood) closed time PDF was $f(t) = 0.64/6.1 \cdot \exp(-t/6.1) + 0.27/18 \cdot \exp(-t/18) + 0.09/48 \cdot \exp(-t/48)$ and a minimum interburst interval of 9.7 ms was calculated from Eq. 2. It was estimated that up to 26% of all the closures were assigned to the wrong category, including roughly equal proportions of the shortest and longest distributions but also a rather larger proportion of intermediate closures. The bins of the histograms in Fig. 5 are obscured by the fitted exponentials.

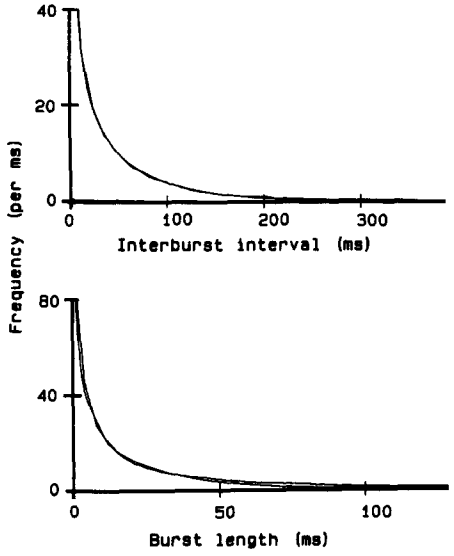

FIGURE 5. Single-channel bursting behavior from a channel activated by 100 μM Ca^{2+}. Histograms of interburst intervals and burst durations (upper and lower traces, respectively) fitted by eye to two exponential components. The minimum burst length was 9.7 ms (see text) and the PDFs are $f(t) = 0.60/12 \cdot \exp(-t/12) + 0.40/57 \cdot \exp(-t/57)$ and $f(t) = 0.69/3.3 \cdot \exp(-t/3.3) + 0.31/23 \cdot \exp(-t/23)$, respectively.

These had two obvious components in each case. The finding that interburst intervals from channels activated by 0.01–100 μM free Ca^{2+} could never be satisfactorily fitted to a single exponential distribution supported earlier inferences of the presence of at least three closed states. Similarly, burst length distributions (as in the lower plot) always contained at least two components, comprising short bursts lasting an average of 2–3 ms, like the shorter openings seen in open-lifetime distributions, and fewer longer bursts.

The distribution of the number of openings per burst was expected to include two main components since lifetime analysis had revealed two open states (Colquhoun and Hawkes, 1982). Because of the very short bursts in the distribution of burst durations, one component was expected to correspond to isolated openings of the brief open state and the other to longer bursts containing more than one opening (and including most of the openings to the longer open state). Examples of the

relevant data collected from bursts of openings of the channel shown in Fig. 5 are presented in Fig. 6 *A*. The frequency distribution has been fitted to two geometric components by the method of maximum likelihood (Fig. 6 *B*). The semilogarithmic plot of log (frequency) vs. openings per burst (Fig. 6 *C*), fitted to the same parameters, may make the double geometric fit more obvious. Similar results were obtained

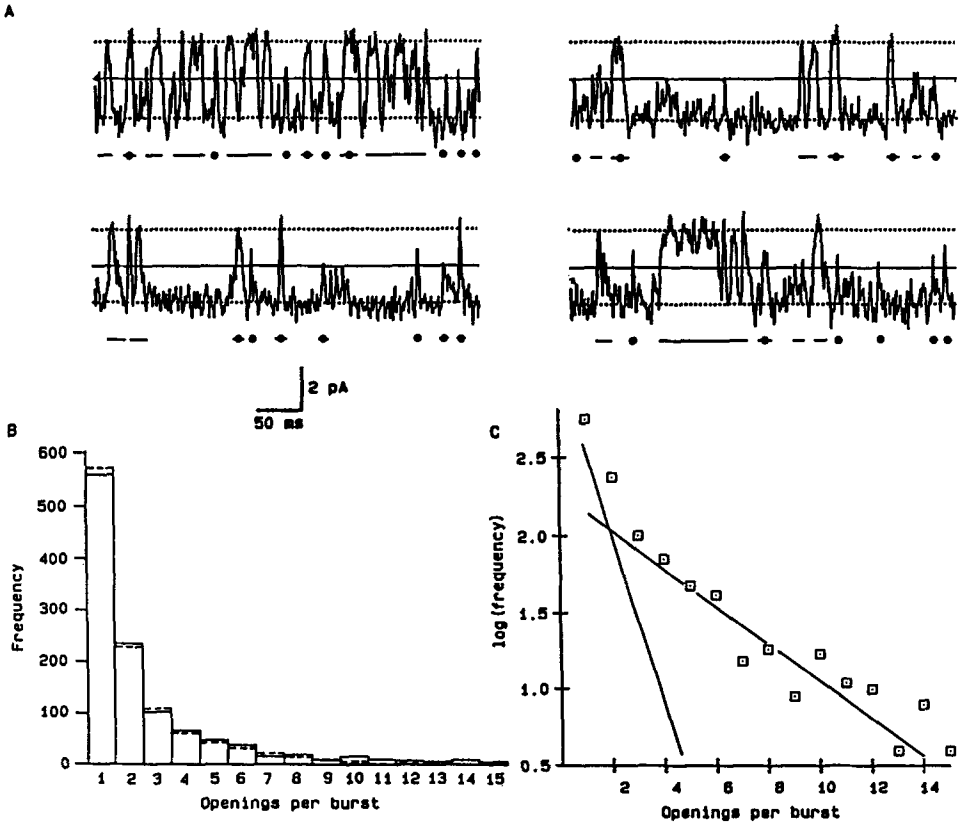

FIGURE 6. Distribution of the number of openings per burst. (Data from the same channel as Fig. 5). (*A*) In these single-channel records the 50% threshold level (*solid horizontal line*) is shown in addition to the open and closed cursor levels. Bursts of openings (threshold crossings separated by the minimum interburst interval of 9.7 ms for this channel) are indicated below each trace and "unit bursts" are marked (●). (*B*) The number of openings in each of 1,159 bursts (*solid bars*) fitted to a double geometric distribution (*dashed bars*) by the method of maximum likelihood: $P(r) = 0.51(1 - 0.27)0.27^{r-1} + 0.49(1 - 0.75)\ 0.75^{r-1}$ (see text). (*C*) Both components of the fitted distribution are superimposed on a semilogarithmic plot of the data.

from several other channels activated by free $[Ca^{2+}]$ as low as 0.01 μM. The "mean number of openings per burst" was obtained from the distributions as $1/(1 - \rho)$, and for Fig. 6 51% of bursts contained a mean of 1.4 openings, while 49% contained a mean of 4.0.

Failure to detect truly unit bursts may reflect frequency limitations, with loss of

many isolated short openings and concatenation of short openings because short gaps were missed. The first problem is more important because even short closures were appreciably longer than short openings (see Table I) and were less likely to be missed. There is no satisfactory method for correcting these multicomponent distributions. However, it can be seen that the overall mean number of openings per burst (2.67) is slightly reduced compared with that derived from the average properties of bursts of openings of this particular channel (where the average number of gaps per burst = $a_s/\Sigma a_l$ = 1.78, whence the average number of openings per burst was 2.78). This may reflect the apparent improvement in resolution when detecting events alone (without needing to resolve their durations) and implies that better resolution could further reduce the overall mean number of openings per burst by the capture of more true unit bursts.

If many bursts actually consisted of single openings to the briefer open-time distribution then "unit bursts" from a given channel should have an appropriate life-

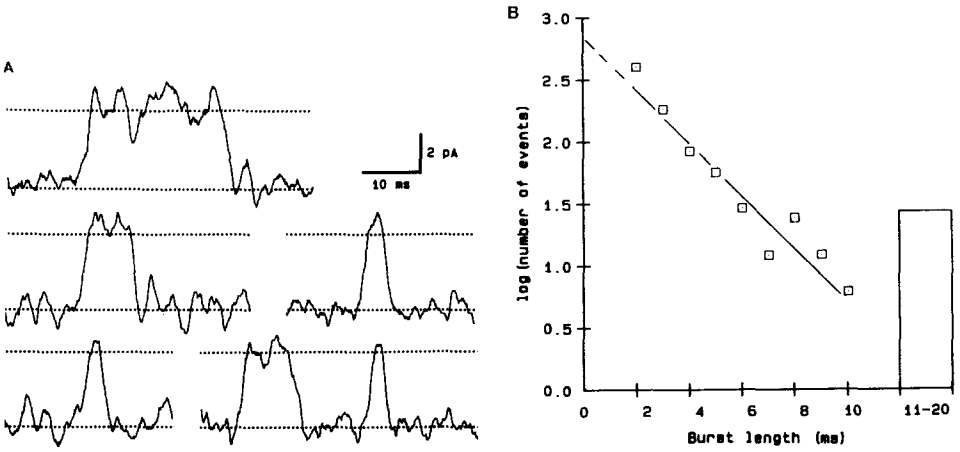

FIGURE 7. Lifetime distribution of unit bursts. (*A*) Examples of unit bursts from the channel illustrated (Figs. 5 and 6). (*B*) Lifetime data fitted (by least squares) to a single line as shown. The few bursts lasting 11–20 ms are grouped together and excluded from the fit.

time distribution. This corollary was tested for several channels and the results for the channel described here are shown in Fig. 7. A minimum burst duration of 2 ms was imposed (as for general lifetime analysis) and 842 unit bursts were collected (some examples of which are presented in Fig. 7 *A*). The semilogarithmic lifetime frequency plot (Fig. 7 *B*) is well fitted (by least-squares) to a straight line, and the time constant is 2.3 ms. The open-time distribution for this channel was $f(t) = 0.91/2.6 \cdot \exp(-t/2.6) + 0.09/14 \cdot \exp(-t/14)$ so the time constant of the shorter-lived open state does appear to correspond to that for the lifetimes constituting unit bursts. However, extrapolation of the fit in Fig. 7 *B* suggests that the distribution actually contained only 703 unit bursts. Because of bandwidth limitations, extrapolation to rather more than the 842 bursts actually counted had been expected. This apparent underestimate was seen with other channels analyzed in this way, and one explanation (which is discussed later) would be that there is another distribution of unit bursts of longer mean lifetime.

Interconnections between Open and Closed States

Routes between open and closed states have been taken to represent isomerization pathways for the channel protein. The presence of more than one pathway may give rise to correlations between successive open (or closed) times (Jackson et al., 1983; Labarca et al., 1985; Kerry et al., 1987, 1988) and also to correlations between neighboring open and closed durations (McManus et al., 1985). That is, if two open states are each connected to different closed states, then the length of successive open times may be correlated because openings will tend to arise repeatedly from the immediately preceding closed state. As events further and further apart are compared, the autocorrelation function (ACF) decays geometrically, the number of components being $1 - N_p$, where N_p represents the number of pathways between the open and closed states (Fredkin et al., 1985).

Both open and closed times were correlated for channels activated by low (0.01 μM), intermediate, or high (100 μM) free [Ca^{2+}]. This is illustrated for the channel

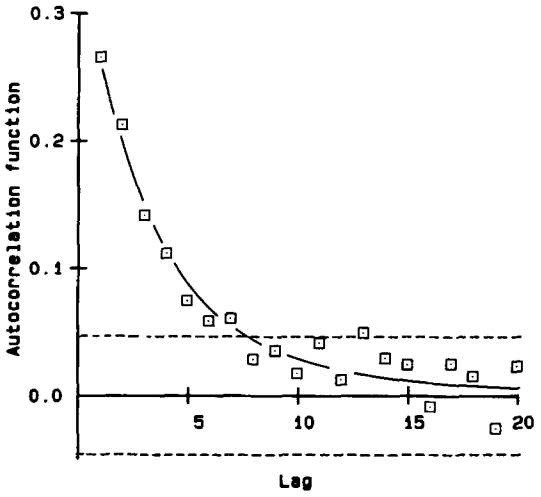

FIGURE 8. Open-time autocorrelation function for up to every 20th opening (lag = 1–20) of the channel shown in Figs. 5–7. The 95% confidence limits for the absence of correlation are shown as dotted lines. The ACF decay is fitted (by least squares) to a single geometric distribution.

already described in Figs. 5–7, for which the ACF decay of 1,792 successive openings is shown in Fig. 8. Events <2 ms long were as usual excluded, but their omission will not have affected the correlations observed (Ball and Sansom, 1988). Similar results were obtained by including all detected events in the anlaysis, which of course gives an artifactual bias towards very short openings (but correlation functions were appreciably less scattered when >2,000 events were examined). Satisfactory fits were obtained with a single geometric component, and the open (and closed) time ACFs were therefore consistent with the existence of two pathways between open and closed states or aggregates. Using the arguments of Colquhoun and Ogden (1986) and denotating all closed states as "F" states and open states as "A" (for "activated") states, then Con(A,F), the connectivity between open and closed states, was 2. Put another way, two states must be abolished to disconnect the open and closed states completely.

Correlations may also arise between the durations of (and the number of openings in) successive bursts (Colquhoun and Ogden, 1986). That is, Con(A,C) > 1,

where C represents long-lived closed states with which A states can communicate directly or via B, for short or "bursting," closed states. For the Ca^{2+} release channel at least, it is possible that Con(A,C) = 1 while Con(A,F) = 2, i.e., the bursting state does not separate C and A states. However, were this to occur, it is hard to conceive of an arrangement whereby a distribution of unit bursts could arise. In fact, direct inspection of the numbers of openings in successive bursts showed obvious clustering of bursts containing more than one opening, but this sort of behavior was less noticeable for burst durations.

Clustering of burst lengths was however revealed by runs analysis of several channels records. Table II shows this applied to a channel activated by only 0.03 μM free [Ca^{2+}]. It was difficult to obtain large numbers of events from channels where P_o was typically 0.01 (see Fig. 2), making standard autocorrelation analysis subject to anomalies and scatter. Yet runs analysis does show nonrandom clustering of burst lengths at just over 3 SDs from the mean ($P < 0.003$). That is, there are so few ways

TABLE II

Runs Analysis

l	No. of runs	n_0	n_1	Z	Significance
ms					
2	158	97	420	−0.09	
4	218	194	323	−2.39	$P < 0.05$
6	236	233	284	−1.87	
8	224	275	242	−3.05	$P < 0.003$
10	231	326	191	−1.03	
12	223	363	154	0.60	
14	167	417	100	0.60	
—	—	—	—	—	
—	—	—	—	—	
26	3	516	1	0.06	
27	1	517	0	—	

Part of the analysis of 517 burst lengths from a channel activated by 0.03 μM Ca^{2+}. The significance level for nonrandom clustering was maximal for the 224 runs produced by choosing a burst length l of 8 ms (which divided the bursts approximately equally between categories 0 and 1).

of accommodating 224 runs with an arbitrary interval length of 8 ms that the finding is highly significant.

Mg^{2+} Inhibition and Lifetime Analysis

The skeletal muscle SR Ca^{2+} release channel conducts large quantities of Mg^{2+} provided the ion is only present on the *trans* (SR lumenal) side of the channel. Smith et al. (1986) reported gMg/gCa = 0.40 with ~50 mM MgHEPES *trans,* where g is the slope conductance (apparently constant at least over holding potentials from −20 to 0 mV). The cardiac channels in this study behaved in a similar fashion (data not shown). However, when Mg^{2+} was added to the *cis* (cytoplasmic or myoplasmic) side of the channel, concentrations of a few millimolar caused a substantial reduction in macroscopic currents (Smith et al., 1986), apparently mainly by reducing P_o (Rousseau et al., 1986). Typical recordings from the cardiac channels studied here are provided in Fig. 9. The normal pattern of channel gating was disrupted with a

marked reduction in the number of openings (which nevertheless could reach the fully open level, Fig. 9 *B*).

Lifetime distributions in the presence and absence of *cis* Mg^{2+}, such as those shown in Fig. 10 *B*, were consistent with an effect on gating. The frequency of openings was gradually decreased by Mg^{2+} added in 0.5–1 mM increments. Open-time distributions continued to be more satisfactorily fitted to two exponential components rather than one ($P < 0.05$), despite the severe reduction in the number of openings for analysis. The proportion of openings to the longer open-time distribution often did appear to be reduced, but as fewer of these longer openings were collected this component approached the limit of detection. Channel closed-time distributions were also altered, in that three components became no more statistically likely than two. This was due to the gradual loss of the very shortest closed-time

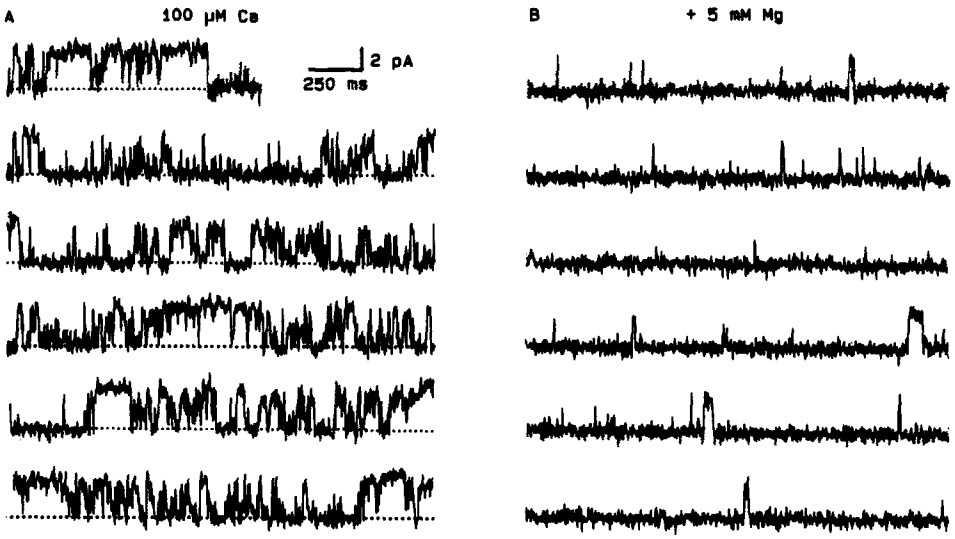

FIGURE 9. Channel records and Mg^{2+}. (*A*) Continuous recording (total 1.9 s) from a single channel activated by 100 μM Ca^{2+}. (*B*) Recorded immediately after adding 5 mM Mg gluconate to the *cis* chamber.

component (corresponding to "gaps within bursts" in the analysis presented earlier). The limited data suggested that the mean lifetime of this component remained unchanged (3–5 ms) while the overall mean closed time, and that of the two longer components, increased.

The effects of Mg^{2+} could not be examined over a very wide range of activating free [Ca^{2+}] (or at [Mg^{2+}] > 5 mM) simply because it was difficult to collect enough events (at least 1,000) to justify any form of lifetime analysis. The possibility of a separate pathway for Mg^{2+} activation was investigated by chelating all the residual Ca^{2+} in the *cis* chamber after incorporating single Ca^{2+}-sensitive channels (calculated free [Ca^{2+}] < 10^{-19} M). This did not completely abolish transitions, which continued to occur at a greatly reduced frequency (as few as two to three per minute), but with normal amplitude. These could have arisen from residual Ca^{2+}-insensitive

activation or a separate class of channels. Additions of up to 1.5 mM Mg gluconate failed to produce any (further) activation, but in all cases reperfusion with Ca^{2+}-containing solutions resulted in a return to normal activity.

The very short mean open time in the presence of *cis* Mg^{2+} was at least as brief as that of the shorter mean open time of the distributions of openings observed under

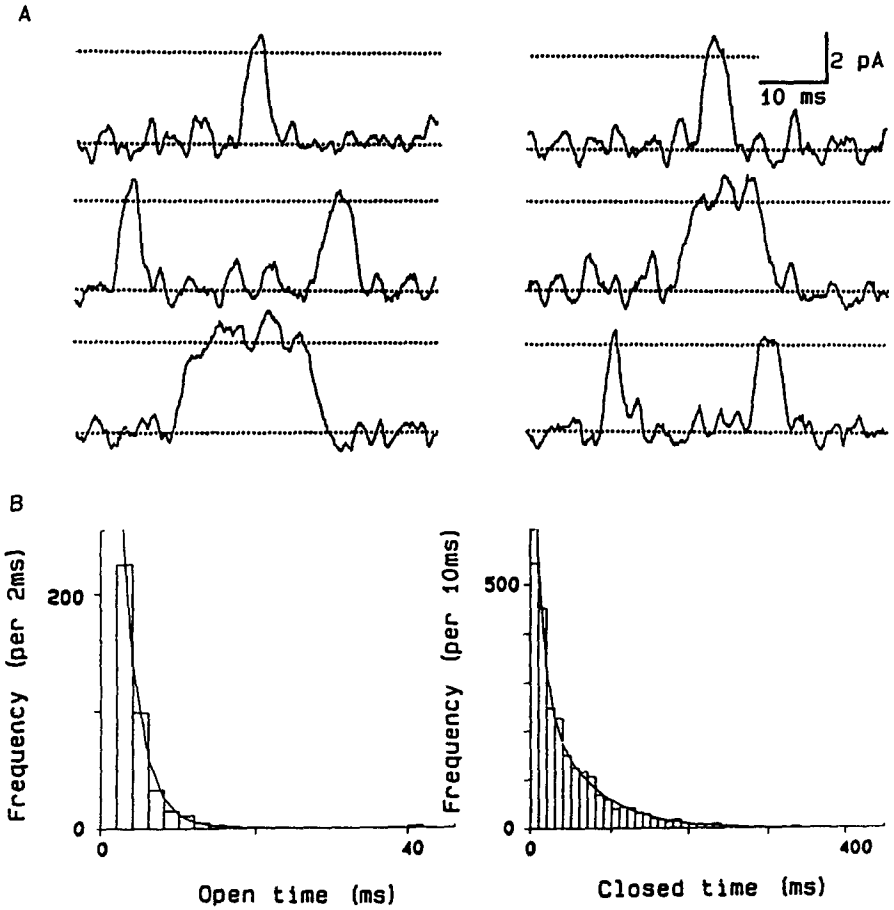

FIGURE 10. Effect of Mg^{2+} on lifetime distributions. For comparison, 5 mM Mg^{2+} was added to the *cis* chamber in the experiment shown in Fig. 3, in the presence of 100 μM Ca^{2+}. (*A*) Single-channel records showing transitions between closed (*lower*) and open (*upper*) levels. (*B*) The open and closed time PDFs are now $f(t) = 0.98/2.3 \cdot \exp(-t/2.3) + 0.02/14 \cdot \exp(-t/14)$ and $f(t) = 0.29/10 \cdot \exp(-t/10) + 0.71/58 \cdot \exp(-t/58)$, respectively (compare with Fig. 3).

normal conditions. As it was already proving difficult to collect enough events for lifetime analysis, fluctuation analysis was used to compare channels in the presence and absence of Mg^{2+}. The bilayers and associated electronics used in these studies contributed a substantial amount of noise to all the recordings, and data were corrected by subtracting noise spectra obtained from the bilayers before channel incor-

poration. It was always possible to superimpose corrected spectra with and without added Mg^{2+} (data not shown) indicating that noise analysis at a bandwidth of 2 kHz (see Methods) was also incapable of demonstrating any definite differences between Ca^{2+}-activated channels with and without *cis* Mg^{2+}.

DISCUSSION

The Ca^{2+} Release Channel Is an Atypical Agonist-activated Channel

Studies with membrane vesicles have identified several agents that affect SR Ca^{2+} release, many acting at distinct and separate sites (Meissner, 1984; Palade, 1987). Previous studies of Ca^{2+} release channels in bilayers have particularly emphasized, the importance of adenine nucleotides for channel activation (Smith et al., 1985, 1986; Rosseau et al., 1986), and caffeine-related compounds also activate the channel (Palade, 1987; Pessah et al., 1987; Ashley and Williams, 1988; but see Meissner, 1984). In this report, experiments were simplified by excluding activators and inhibitors other than Ca^{2+} and Mg^{2+}, but with Ca^{2+} as the sole agonist only generally low P_o values were achieved.

Agonist-activated channels from cell surface membranes have, as a group, much in common. The primary structures of the nicotinic acetylcholine receptor, the $GABA_A$ receptor and the glycine receptor, are very similar (Stevens, 1987), and all the agonist-activated channels best studied at the single-channel level—the nicotinic acetylcholine receptor (Colquhoun and Sakmann, 1985), the glutamate receptor (Kerry et al., 1988), and the large-conductance Ca^{2+}-activated K^+ channel (Magleby and Pallotta, 1983; Moczydlowski and Latorre, 1983)—show marked cooperativity of agonist activation. The Ca^{2+} release channel has functional features more in common with gap-junction channels (Ma et al., 1988; Smith et al., 1988) and its behavior with Ca^{2+} is also quite distinct in that the relationship between activating free [Ca^{2+}] and P_o is decidedly sublinear. This tends to exclude standard cooperative models for channel gating (at least with Ca^{2+} as the sole agonist), which would envisage Ca^{2+} binding sequentially to several sites on the channel protein to induce various open states.

Multiple States and the Site of Ca^{2+} Interaction

After the usual Markov assumptions there is good evidence that the SHSR channel can exist in several kinetically distinguishable states. This study counted more closed states than Smith et al. (1986) or Rousseau et al. (1986), who made the first proposals for a kinetic scheme. There are a minimum of three closed and two open states, as judged from the minimum numbers of exponential components required to fit lifetime distributions (and the durations of interburst intervals) as well as the presence of two geometric components in the distributions of the numbers of openings per burst. Given the rather limited time resolution (a dead time of 1 ms) this picture is likely to be incomplete, and yet more reasons for missing lifetime components have been mentioned earlier. On the other hand, frequency limitations do not introduce wholly fictitious states as long as measured lifetimes are at least twice the dead time (Roux and Sauvé, 1985; Blatz and Magleby, 1986*b*), although of course mean lifetimes will be prolonged if short interruptions are undetected.

The conformations of closed (nonconducting) and open (conducting) channels must obviously differ, and the very rapid and unresolved transitions between relatively long-lived open and closed states supports the usual assumption that they represent relatively stable isomers (or groups of isomers) of the channel protein. Multiple closed or open states are usually accorded the same status, but it may be impossible to identify individual states (and presumed different conformations) from the experimental record. No differences were found between open-state conductances at this resolution. The closed states similarly could only be identified in statistical terms, with the Markov assumptions that transition rates are time independent (constant) and states are memoryless. Thus, even though Ca^{2+} reduces the mean durations of all three closed states, the ion need interact with only one closed state to have this effect if the states cannot be distinguished from each other in the recordings.

The bursting behavior of the channels and the correlation between successive open (and closed) times and burst lengths allowed strong inferences to be made about the ways in which the various states were interconnected, and which state (and therefore possibly which conformation) might bind Ca^{2+}. Although no assumptions were made about the molecular mechanisms involved, and the bursting behavior of the channels was only defined after statistical analysis, two main constraints became clear. Firstly, a pathway must exist for open-closed transitions giving rise to isolated single openings to, apparently, the shorter-lived open state. Secondly, the gating pathway cannot be arranged in a simple linear scheme because the lifetime correlations require the existence of (at least) two pathways between open and closed states. This excludes the general scheme:

$$C \rightleftharpoons C \rightleftharpoons C \rightleftharpoons O \rightleftharpoons O \qquad \text{(Scheme 1)}$$

It should be noted that the original mechanism proposed for skeletal SR channels by Smith et al. (1986) must be nested within this scheme when Ca^{2+} binding controls the only pathway for channel activation. This general scheme is also incompatible with the discovery of correlations between successive burst lengths and the numbers of openings per burst, which also allow the definite exclusion of schemes such as:

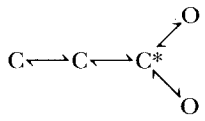

(Scheme 2)

where C* is a single gateway state (Fredkin et al., 1985) between open and closed conformations.

Minimal Kinetic Schemes for Ca^{2+} Activation

One aspect of Ca^{2+} activation that emerged from this study was that the number of short and long openings (strictly, openings to the short and long distributions) were increased to the same extent by Ca^{2+}. Letting the channel open directly to either of the open states, which is consistent with this observation, and further assuming that Ca^{2+} acts early in the activation pathway of the Ca^{2+} release channel, leads to a

cyclical or branched gating scheme such as:

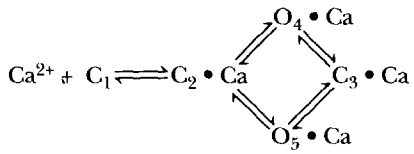

(Scheme 3)

Schemes modelled on that for the acetylcholine receptor, the glutamate receptor, or the Ca^{2+}-activated K^+ channel, which are all subsets of the general scheme,

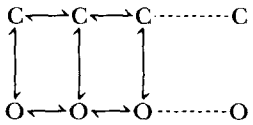

(Scheme 4)

with agonist molecules binding mainly to closed states but also to open states (Moczydlowski and Latorre, 1983), cannot easly be applied to the SHSR channel mainly because it is difficult to allocate sites for cation binding that do not favor the occurrence of certain open states. Even for acetylcholine receptors there is an excess of short openings which cannot be accounted for within the general model (Colquhoun and Sakmann, 1985; Sine and Steinbach, 1986).

Scheme 3 permits single isolated openings to either open-time distribution, now attributed to specific open states. Of course, at this resolution "openings" may in fact be bursts of openings (with unresolved very short closures), and the open states may turn out to be aggregates of openings. Nevertheless this state diagram would remain a valid summary of the experimental findings, and could be tested further. Specifically, although >90% of all openings are to the short open-time distribution (O_4 say), there is also a pathway for "long" unit bursts, but without collecting large numbers of events they would be overlooked. This may have occurred; see for example Fig. 7 *B*, where at least 15% of the unit bursts were apparently unaccounted for. Some of these may have comprised the required distribution with a longer mean lifetime, and long recordings lasting 10–20 min, under good conditions, will be needed to answer this question. These requirements may be met by reconstituting the purified channels into liposomes for patch-clamping (Tank and Miller, 1982; Tomlins and Williams, 1986).

Correlations between successive open times are explained on the basis that openings could arise either from the reaction $C_2 \cdot Ca^{2+} \rightleftharpoons O_{4/5} \cdot Ca$ or via $C_3 \cdot Ca \rightleftharpoons O_{4/5} \cdot Ca$. There may be other schemes consistent with the data, including particularly those where openings may arise from long-lasting closed states, "gaps within bursts" representing periods of a few milliseconds (on average) spent in more distal closed states. If Ca^{2+} can also "inactivate" the channel at higher concentrations (Smith et al., 1986), this could be accomodated by postulating closed states further along the activation pathway (beyond $C_3 \cdot Ca$ in scheme 3), or "self-blocked" states.

Mg^{2+} and Channel Inhibition

The possibility that Mg^{2+} might block the skeletal channel was briefly considered by Smith et al. (1986). The results reported here (using relatively low concentrations of

Mg^{2+}) are clearly inappropriate for either very slow or very fast block by Mg^{2+} (Hille, 1984), but the slight "flickery" appearance was not incompatible with an intermediate type of block where Mg^{2+} binds to a site in the channel conduction pathway for an average of 1 or 2 ms (Yellen, 1984). A problem arises in that it is difficult to explain why Mg^{2+} should be so permeant in one direction (*trans-cis*) but not when entering from the *cis* side. The channel would need to have very substantially different energy profiles in response to the sideness of Mg^{2+}. Extreme coupling of protein conformation to (ion) transport is of course one mechanism for a membrane carrier (Läuger, 1985). Although channel and carrier mechanisms are not mutally exclusive, further analysis did seem to show that the effect of *cis* Mg^{2+} was understandable in terms of channel gating and the activation pathway.

To agree with the competition model for the effect of Mg^{2+} on SR Ca^{2+} release (Meissner et al., 1986; Meissner and Henderson, 1987; Smith et al., 1986), Mg^{2+} must compete with Ca^{2+} for a divalent cation binding site on, for example, state C_1 in scheme 3. The Mg channel complex either cannot open at all or opens slowly (i.e., infrequently) to a new short-lived open state (or states). In this latter case, there should be multiple open-time distributions with both Ca^{2+} and Mg^{2+} present, which were not seen. Also, a certain degree of activation should occur with Mg^{2+} alone, but the appropriate tests failed to reveal any. The open lifetimes that could be measured seemed to be similar to those seen with Ca^{2+} activation. Scheme 3 could thus be slightly modified:

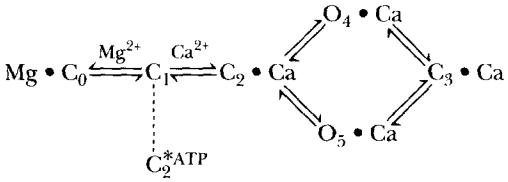

(Scheme 5)

State $C_3 \cdot Ca$ in schemes 3 or 5 must represent a relatively long-lived closed state which is needed to terminate the unit bursts seen with Ca activation. State $C_2 \cdot Ca$ must be a short-lived "bursting" state. The new nonconducting state $Mg \cdot C_0$, together with C_1, becomes increasingly important as $[Mg^{2+}]$ is increased. Activators like ATP may bind to C_1 at other sites (*) to produce multiply liganded channel complexes which are able to give rise to new open-time distributions.

The ryanodine-receptor/Ca^{2+} release channel complex is an unusually large membrane protein (~400 kD per oligomer, Imagawa et al., 1987; Lai et al., 1988*a*) with several distinct ligand-binding sites and possibly a major structural role in terminal and junctional SR. Evidence is emerging for a more widespread distribution of similar channel proteins in tissues other than striated muscle (Ashley, 1989). Although they probably operate in multichannel arrays, even a preliminary analysis of single channels at 2 ms resolution has revealed suitably complicated kinetics. The channel also displays multiple subconductance states (which were deliberately not investigated here). At one level these may represent interactions between oligomers (Ma et al., 1988) but fast, hidden sublevels could influence ion permeation, and the flow of ions could affect gating (Läuger, 1985). A nonequilibrium system should fail to show microscopic reversibility, and under some conditions it may be possible to

demonstrate new clockwise or anticlockwise cycling around the gating schemes suggested here. Some of these predictions are now being tested.

R.H. Ashley was supported by a Wellcome Trust Research Training Fellowship in Mental Health, and A.J. Williams was supported by the British Heart Foundation.

Original version received 10 June 1988 and accepted version received 11 September 1989

REFERENCES

Ashley, R. H. 1989. Activation and conductance properties of ryanodine-sensitive calcium channels from brain microsomal membranes incorporated into planar lipid bilayers. *Journal of Membrane Biology.* 111:179–189.

Ashley, R. H., and A. J. Williams. 1988. Activation of the sheep cardiac muscle sarcoplasmic reticulum membrane Ca^{2+} channel by AR-L 115 (Sulmazole). *Journal of Physiology.* 406:213p. (Abstr.)

Ball, F. G., and M. S. P. Sansom. 1988. Single-channel autocorrelation functions: the effects of time interval omission. *Biophysical Journal.* 53:819–832.

Blatz, A. L., and K. L. Magleby. 1986*a*. A quantitative description of three modes of activity of fast chloride channels from rat skeletal muscle. *Journal of Physiology.* 378:141–174.

Blatz, A. L., and K. L. Magleby. 1986*b*. Correcting single-chanel data for missed events. *Biophysical Journal.* 49:967–980.

Blinks, J. R., W. G. Wier, P. Hess, and F. G. Prendergast. 1982. Measurement of Ca^{2+} concentrations in living cells. *Progress in Biophysics and Molecular Biology.* 40:1–114.

Colquhoun, D., and A. G. Hawkes. 1982. On the stochastic properties of bursts of single ion channel openings and clusters of bursts. *Philosphical Transactions of the Royal Society London B.* 300:1–59.

Colquhoun, D., and D. C. Ogden. 1986. States of the nicotinic acetylcholine receptor. Enumeration, characteristics and structure. *In* NATO ASI Series Vol H3. Springer-Verlag. Berlin.

Colquhoun, D., and B. Sakmann. 1985. Fast events in single channel currents activated by acetylcholine and its analogues at the frog muscle end-plate. *Journal of Physiology.* 369:501–557.

Colquhoun, D., and F. J. Sigworth. 1983. Fitting and statistical analysis of single-channel recording. *In* Single-channel recording. B. Sakmann and E. Neher, editors. Plenum Publishing Corp., New York. 191–263.

Endo, M. 1981. Mechanism of Ca^{2+}-induced Ca^{2+} release in the sarcoplasmic reticulum membrane. *In* Mechanisms of Gated Ca^{2+} Transport across Biological Membranes. S. T. Ohnishi and M. Endo, editors. Academic Press, New York. 257–264.

Finkelstein, A., J. Zimmerberg, and F. S. Cohen. 1986. Osmotic swelling of vesicles: its role in the fusion of vesicles in planar phospholipid bilayer membranes and its possible role in exocytosis. *Annual Review of Physiology.* 48:163–174.

Fredkin, D. R., M. Montal and J. A. Rice. 1985. Identification of aggregated Markovian models: application to the nicotinic acetylcholine receptor. *In* Proceedings of the Berkley Conference in Honour of Jerzy Neyman and Jack Kiefer. Vol. 1. M. LeC. Lucien and R. A. Olshen, editors. Wadsworth, Belmont. 269–289.

Hille, B. 1984. Ionic Channels of Excitable Membranes. Sinauer Associates, Inc., Sunderland, MA. 426 pp.

Horne, R., and K. Lange. 1983. Estimating kinetic constants from single-channel data. *Biophysical Journal.* 43:207–223.

Imagawa, T., J. S. Smith, R. Coronado, and K. P. Campbell. 1987. Purified ryanodine receptor

from skeletal muscle sarcoplasmic reticulum is the Ca^{2+}-permeable pore of the Ca^{2+} release channel. *Journal of Biological Chemistry.* 262:16636–16643.

Jackson, M. B., B. S. Wong, C. E. Morris, H. Lecar, and C. N. Christian. 1983. Successive openings of the same acetylcholine receptor channel are correlated in open time. *Biophysical Journal.* 42:109–114.

Kerry, C. J., K. S. Kits, R. C. Ramsey, M. S. P. Sansom, and P. N. R. Usherwood. 1987. Single channel kinetics of a glutamate receptor. *Biophysical Journal.* 51:137-144.

Kerry, C. J., R. C. Ramsey, M. S. P. Sansom, and P. N. R. Usherwood. 1988. Glutamate receptor channel kinetics. The effect of glutamate concentration. *Biophysical Journal.* 53:39–52.

Labarca, P., J. A. Rice, D. R. Fredkin, and M. Montal. 1985. Kinetic analysis of channel gating. Application to the cholinergic receptor channel and the chloride channel from Torpedo californica. *Biophysical Journal.* 47:469–478.

Lai, F. A., H. P. Erickson, E. Rousseau, Q.-Y. Liu, and G. Meissner. 1988*a*. Purification and reconstitution of the Ca^{2+} release channel from skeletal muscle. *Nature.* 331:315–319.

Lai, F. A., H. P. Erickson, E. Rousseau, Q.-Y. Liu, and G. Meissner. 1988*b*. Evidence for a Ca^{2+} channel within the ryanodine receptor complex from cardiac sarcoplasmic reticulum. *Biochemical and Biophysical Research Communications.* 151:441–449.

Läuger, P. 1985. Ionic channels with conformational substates. *Biophysical Journal.* 47:581–591.

Liebovitch, L. S., J. Fischbarg, J. P. K. Koniarek, I. Todorova, and M. Wang. 1987. Fractal model of ion channel kinetics. *Biochimica et Biophysica Acta.* 896:173–180.

Lowry, O. H., N. J. Rosebrough, D. L. Farr, and R. J. Randall. 1951. Protein measurements with Folin-phenol reagent. *Journal of Biological Chemistry.* 193:265–275.

Ma, J., M. Fill, M. Knudson, K. P. Campbell, and R. Coronado. 1988. Ryanodine receptor of skeletal muscle is a gap junction-type channel. *Science.* 242:99–102.

Magleby, K. L., and B. S. Pallotta. 1983. Ca dependence of open and shut interval distributions from Ca-activated potassium channels in cultured rat muscle. *Journal of Physiology.* 344:585–604.

McManus, O. B., A. L. Blatz, and K. L. Magleby. 1985. Inverse relationship of the durations of adjacent open and shut intervals for chloride and potassium channels. *Nature.* 317:615–627.

Meissner, G. 1984. Adenine nucleotide stimulation of Ca^{2+}-induced Ca^{2+} release in sarcoplasmic reticulum. *Journal of Biological Chemistry.* 259:2365–2374.

Meissner, G., E. Darling, and J. Eveleth. 1986. Kinetics of rapid Ca^{2+} release by sarcoplasmic reticulum. Effects of Ca^{2+}, Mg^{2+} and adenine nucleotides. *Biochemistry.* 25:236–244.

Meissner, G., and J. S. Henderson. 1987. Rapid Ca^{2+} release from cardiac sarcoplasmic reticulum vesicles is dependent on Ca^{2+} and is modulated by Mg^{2+}, adenine nucleotide and calmodulin. *Journal of Biological Chemistry.* 262:3065–3073.

Miller, C., and E. Racker. 1976. Calcim-induced fusion of fragmented sarcoplasmic reticulum with artificial planar bilayers. *Journal of Membrane Biology,* 30:283–300.

Miller C., and R. L. Rosenberg. 1979. A voltage-gated cation conductance channel from frog sarcoplasmic reticulum. *Biochemistry.* 18:1138–1145.

Moczydlowski, E. 1986. Single-channel enzymology. *In* Ion Channel Reconstitution. C. Miller, editor. Plenum Publishing Corp., New York. 75–113.

Moczydlowski, E., and R. Latorre. 1983. Gating kinetics of Ca^{2+}-activated K^+ channels from rat muscle incorporated into planar lipid bilayers. Evidence for two voltage-dependent Ca^{2+} binding reactions. *Journal of General Physiology.* 82:511–542.

Palade, P. 1987. Drug-induced Ca^{2+} release from isolated sarcoplasmic reticulum II: releases involving a Ca^{2+}-induced Ca^{2+} release channel. *Journal of Biological Chemistry.* 262:6142–6148.

Pessah, I. N., R. A. Stambuk, and J. E. Casida. 1987. Ca^{2+}-activated ryanodine binding: mecha-

nisms of sensitivity and intensity modulation by Mg^{2+}, caffeine and adenine nucleotides. *Molecular Pharmacology.* 31:232–238.

Rousseau, E., J. S. Smith, J.S. Henderson, and G. Meissner. 1986. Single channel and $^{45}Ca^{2+}$ flux measurements of the cardiac sarcoplasmic reticulum calcium channel. *Biophysical Journal.* 50:1009–1014.

Rousseau, E., J. S. Smith, and G. Meissner. 1987. Ryanodine modifies conductance and gating behavior of single Ca^{2+} release channel. *American Journal of Physiology.* 253:C364–368.

Roux, B., and R. Suavé. 1985. A general solution to the time interval omission problem applied to single channel analysis. *Biophysical Journal.* 48:149–158.

Schneider, M. F., and W. K. Chandler. 1973. Voltage dependent charge movement in skeletal muscle: a possible step in excitation-contraction coupling. *Nature.* 242:244–246.

Sigworth, F. J. 1983. Electronic design of the patch clamp. *In* Single-Channel Recording. B. Sakmann and E. Neher, editors. Plenum Publishing Corp., New York. 3–35.

Sine, S. M., and J. H. Steinbach. 1986. Acetylcholine receptor activation by a site-selective ligand: nature of brief open and closed states in BC3H-1 cells *Journal of Physiology.* 370:357–379.

Smith, J. S., R. Coronado, and G. Meissner. 1985. Sarcoplasmic reticulum contains adenine nucleotide-activated calcium channels. *Nature.* 316:446–449.

Smith, J. S., R. Coronado, and G. Meissner. 1986. Single channel measurements of the calcium release channel from skeletal muscle sarcoplasmic reticulum. *Journal of General Physiology.* 88:573–588.

Smith, J. S., T. Imagawa, J. Ma, M. Fill, K. P. Campbell, and R. Coronado. 1988. Purified ryanodine receptor from rabbit skeletal muscle is the calcium-release channel of sarcoplasmic reticulum. *Journal of General Physiology.* 92:1–26.

Stevens, C. F. 1987. Channel families in the brain (commentary). *Nature.* 328:198–199.

Tanifuji, M., M. Sokabe, and M. Kasai. 1987. An anion channel of sarcoplasmic reticulum incorporated into planar lipid bilayers. Single channel behavior and conductance. *Journal of Membrane Biology.* 99:103-111.

Tank, D. W., and C. Miller. 1982. Isolated-patch recording from liposomes containing functionally reconstituted chloride channels from *Torpedo* electroplax. *Proceedings of the National Academy of Sciences.* 79:7749–7753.

Tomlins, B., and A. J. Williams. 1986 Solubilisation and reconstitution of the rabbit skeletal muscle sarcoplasmic reticulum K^+ channel into liposomes suitable for patch clamp studies. *Pflügers Archiv.* 407:341–347.

Volpe, P., G. Salviati, F. Di Virgilio, and T. Pozzan. 1985. Inositol 1,4,5-trisphosphate induces Ca^{2+} release from sarcoplasmic reticulum of skeletal muscle. *Nature.* 316:347–349.

Woodbury, D. J., and J. E. Hall. 1988. Role of channels in the fusion of vesicles with a planar bilayer. *Biophysical Journal.* 54:1053–1063.

Yellen, G. 1984. Ionic permeation and blockade in Ca^{2+}-activated K^+ channels of bovine chromaffin cells. *Journal of General Physiology.* 84:157–186.